

MULTILEVEL BLOCK MATCHING TECHNIQUE WITH THE USE OF GENERALIZED PARTIAL VOLUME INTERPOLATION FOR NONLINEAR INTERSUBJECT REGISTRATION OF MRI BRAIN IMAGES

Daniel Schwarz and Tomas Kasparek

Institute of Biostatistics and Analyses, Masaryk University
Kamenice 3, 625 00, Brno, Czech Republic
phone: + (420) 549492854, fax: + (420) 549492855, email: schwarz@iba.muni.cz
web: www.iba.muni.cz

ABSTRACT

Spatial normalization of MRI brain images by nonlinear image registration is an essential task for many applications in the field of computational neuroanatomy. Here, a multilevel block matching technique adapted to the problem of intersubject registration is presented. The concept of generalized partial volume (GPV) interpolation, which was originally used in joint intensity histogram computation, is used here in regional similarity matching. The influence of kernel function selected for GPV interpolation on the quality of registration is studied in experiments which include simulated brain images and synthetic deformations.

1. INTRODUCTION

Image registration methods play an important role in the field of computational neuroanatomy. They are used for spatial normalization, voxel-based and deformation-based morphometry, atlas-based segmentation or brain atlas construction. In many of those tasks, registration methods with the use of multimodal similarity measures and nonrigid transformations models are required [1]. Whereas the mutual information is regarded in literature [2] as the standard similarity measure for multimodal image registration, the choice of a deformation model still remains dependent on a specific registration task. Two major classes of locally adaptive transformations are used in medical image registration: parametric transformations, which use a set of corresponding control points or landmarks to compute a piecewise interpolated displacement field [3], [4], and nonparametric transformations, which apply a smoothing operator on a dense field of forces estimated independently in every voxel of the image [5], [6].

Besides the similarity measure and the deformation model, an interpolation method is another basic block of any registration algorithm. Voxel intensities at nongrid positions are interpolated as weighted sums of voxel intensities at neighbouring grid positions. The weights are determined by interpolation kernel functions. In general, higher-order interpolation methods with a larger support lead to smaller intensity errors in the interpolated image. However, it has been shown in [7], that these interpolators do not always ensure also higher registration accuracy, especially in the case of mutual-information-based registration. To alleviate problems

with direct intensity interpolators, partial volume interpolation was proposed in [8] and it was further extended into the generalized partial volume (GPV) interpolation in [9].

In this paper, the effect of various kernel functions in the GPV interpolation is studied on the quality of registration. MRI brain images are registered with an algorithm which incorporates similarity measure derived from mutual information and a spatial deformation model based on radial basis functions (RBF).

2. METHODS

Intersubject and subject-to-atlas registration of in automated morphometry of MRI brain images are the considered applications of algorithms presented here. Thus, the registration method should be capable to capture local subtle anatomical variations as well as global large shape differences. Further, the method should be robust to tissue intensity variations which can be result of multimodality imaging as well as neuropsychological diseases or even normal aging [10]. Recently, a method for multimodal deformable registration in stereotaxic space was proposed in [6]. The registration method, which is considered here, differs from the one in [6] mainly in the spatial deformation model.

2.1 GPV interpolation in multilevel block matching

The scheme of the algorithm is in Fig. 1. A multilevel subdivision is applied on a floating image N . Obtained rectangular image blocks are matched with a reference image M . The resulting displacement field \mathbf{u} is made up from local translations of the image blocks by RBF interpolation. The translations representing warping forces \mathbf{f} are found by maximizing symmetric regional similarity measures.

The concept of regional matching is adapted here from [11]:

$$S_W(\mathbf{w}) = \frac{1}{K_W} \sum_{\mathbf{x} \in W} S_{PMI}(\mathbf{x}) \quad (1)$$

and the region similarity measure S_W is computed in an image region W with the center point \mathbf{w} with K_W voxels by averaging the point similarities over W . The point similarity function S_{PMI} derived from mutual information in [6] is used here:

$$S_{PMI}(\mathbf{x}) = \frac{p_{MN}(m(\mathbf{x}), n(\mathbf{x}))}{p_M(m(\mathbf{x}))p_N(n(\mathbf{x}))}, \quad (2)$$

where $p_M(m)$ and $p_N(n)$ are marginal PDF and $p_{MN}(m,n)$ is the joint PDF of the images M and N respectively. A combined estimate of the joint PDF made from an estimate based on tissue probability maps in stereotaxic space and from an estimate based on the joint intensity histogram is used here. It was shown in [6] that the combined estimate improves the quality of registration.

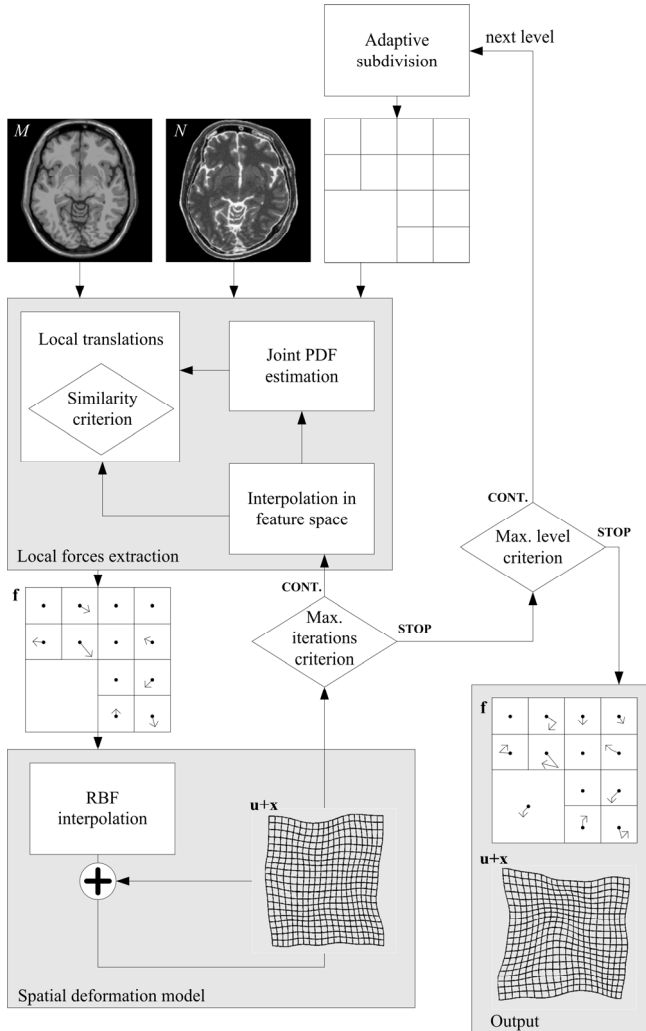


Figure 1 – The scheme of the multilevel block matching technique. The displacement field \mathbf{u} which transforms the floating image N to match the reference image M is searched in an iterative process which involves regional similarity matching and piecewise interpolation with the use of Wendland’s radial basis function.

Due to the subvoxel accuracy of performed deformations, the point similarities have to be computed in points that are not positioned on the image grid. Interpolation from neighboring grid points has to be involved. The function S_{PMI} is defined for a finite number of intensity values due to histogram binning performed in the joint histogram computation. Conventional interpolation of voxel intensities is therefore inapplicable, because the point similarity functions are not defined for new values which would arise. Thus, the GPV interpolation scheme, which was originally designed for computation of joint intensity histogram, is used here. The computation of point pair similarity requires knowledge of the

intensities m and n in the points of the images M and N respectively. The intensity n on a grid point of the deformed grid of the floating image is straightforward, whereas the intensity m on a point off the regular grid of the reference image is unknown. Their similarity is computed as a linear combination of similarities of intensity pairs corresponding to the points in the neighbourhood of the examined point. The extent of the neighbourhood depends on the chosen kernel function. Here, the first-order, the second-order and the third-order B-spline functions with 8, 27 and 64 grid points in neighbourhood for 3-D tasks or 4, 9 and 16 points in neighbourhood for 2-D tasks are used. The particular choice of the kernel function affects the smoothness of the behaviour of the regional similarity measure, see Fig. 2. The number of local optima is the lowest in the case of the third-order B-spline. As the evaluation of the B-splines increases the computational load, their values are computed only once and stored in a lookup table with increments equal to 0.001.

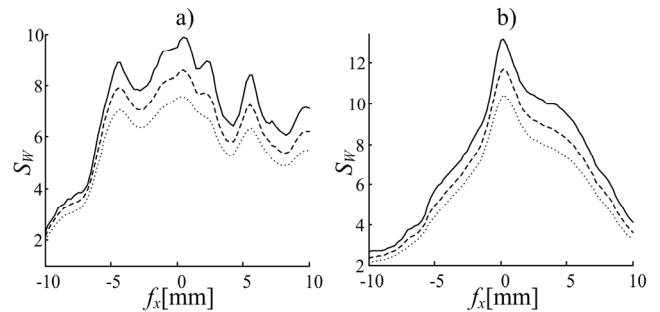


Figure 2 – Comparison of the regional similarity measure computed with the use of GPV and the first-order B-spline (solid line), the second-order B-spline (dashed line) and the third-order B-spline (dotted line). A region of the size a) 10x10 mm, b) 20x20 mm was translated by $f_x = \pm 10$ mm in the x direction.

The central idea to the block matching technique is to locally transform regions of the floating image to match them to the reference image. Local translations which maximize the regional similarity measure S_W are searched in an optimization procedure. Fig. 2b shows that the use of the regional similarity measure and the GPV interpolation with the use of the second-order B-spline or the third-order B-spline leads to well-behaved criterion function in the case of large regions. In the case of small regions, the uncertainty about the best translation is still high and many local maxima occur near the optimal solution, see Fig. 2a. A combination of extensive search and hillclimbing algorithms is used here to find the global maximum. First, a space of all possible translations is determined by absolute maximum translation $|\mathbf{f}_{max}|$ in all directions. Then, the space of all possible translations is searched with a relatively big step s_e . The q best points are then used as starting points for the following hillclimbing with a finer step s_h . The maximum of q local maxima obtained by the hillclimbing is then declared as the global maximum, see Fig. 3. All the parameters of the optimization procedure depend on the size of the region which is translated. In this way, fewer criterion evaluations are done for larger regions when the chance of getting trapped into local

maxima is reduced and more evaluations of the criterion is performed for smaller regions.

Once the local translations are found, the displacement \mathbf{u} is computed separately for each of D dimensions by interpolation with the use of RBF by:

$$u_k(\mathbf{x}) = \sum_{i=1}^B (\alpha_i \cdot R(\|\mathbf{x} - \mathbf{w}_i\|)), \quad k=1\dots D, \quad (3)$$

where $u_k(\mathbf{x})$ is the displacement of a grid point \mathbf{x} in the k^{th} dimension, R is the radial basis function of the distance $\|\mathbf{x} - \mathbf{w}_i\|$ between the grid point \mathbf{x} and the center of the i^{th} block \mathbf{w}_i . The coefficients α_i are computed by putting the translations \mathbf{f} into (3) and solving the resulting linear system of B equations separately for each dimension k . The compactly supported Wendland's RBF, which was successfully used for landmark-based deformable registration in [12], is used here. Its mathematical properties hold for different spatial support which is important for the multilevel strategy. For each level of subdivision, the block size is set to the half of the size at the previous level. The displacements are gradually incremented over all levels, refining the resulting deformation in the coarse-to-fine manner. The regions containing poor contour or surface information can be eliminated from the matching process and the algorithm can be accelerated in this way. The subdivision is performed only if at least one voxel in the current region has its normalized gradient image intensity bigger than a certain threshold.

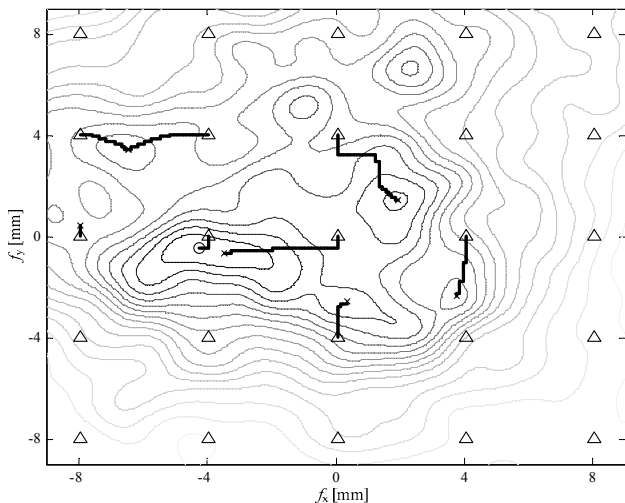


Figure 3 - A trajectory of 2D optimization performed by an extensive search (triangles) combined with hillclimbing (bold lines). The optimization procedure was set for this illustration as follows: $|\mathbf{f}_{\text{max}}|=[8, 8]$, $s_e=4$ mm, $s_h=0.1$ mm, $q=8$. The local maxima are marked by crosses and the global one is marked by the circle.

Optimal matches can be hardly found in a single pass composed of the local translations estimation and the RBF-based interpolation, since features in one location influence decisions at other locations of the images. Iterative updating scheme is therefore proposed here, see Fig. 1. It helps to model better the voxel interdependencies, because the dependency on neighbouring displacements is involved in this way. A preset number of iterations is used as the criterion of termination of the iterative process. The space of all possible translations determined by $|\mathbf{f}_{\text{max}}|$ is divided into proportionally

smaller parts, since the displacement field is updated in an incremental way. The use of the iterative scheme is illustrated in Fig. 4, where the gradual change in local translations through iterations can be observed. An important part in the each iteration is re-computation of the point similarity function before regional matching is performed.

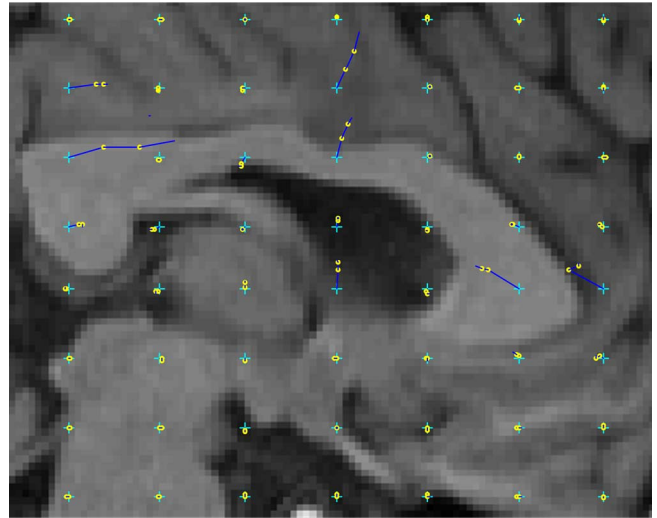


Figure 4 - The iterative estimation of local translations in a synthetically deformed part of an image. The final displacements are sums of partial updates computed by interpolation of the local translations. The magnitude of the translations is scaled by factor 3 for illustration purposes.

2.2 Synthetic deformations

The quality of the registration method with various setups in GPV interpolation is assessed here on recovering synthetic deformations in a lot of registration experiments. The synthetic deformations are produced here by two completely different anatomical variability simulators: 1) RGsim based on Rogelj's elastic-incremental model with Gaussian spatial filters and 2) TPSsim based on thin-plate splines; see [6] for their detailed description. The deformations produced by RGsim are more complex than the smooth TPSsim ones.

3. RESULTS

The optimal setup of the multilevel block matching technique was found experimentally. Values of the method's parameters are listed in Tab. 1.

Table 1 – Setup of the parameters of the multilevel block matching technique.

Level	region size [mm ²]	s [mm]	$ \mathbf{f}_{\text{MAX}} $ [mm]	s_e [mm]	s_h [mm]	q [-]
1	112^2	168	28	2.5	0.50	1
2	56^2	84	14	2.0	0.25	2
3	28^2	42	7	1.5	0.20	2
4	14^2	21	4	1.5	0.20	3
5	7^2	11	2	1.0	0.10	4

The maximum level of subdivision was set to 5 based on preliminary results. This level corresponds to the subimage size of 7x7 pixels. Although the next level of subdivision gave an increase in the global mutual information, the alignment expressed by quantitative evaluation measures, which are described further, and also by visual inspection was constant or worse.

Due to the computational complexity of the registration methods, the quantitative evaluation was done on 2-D data. Both anatomical variability simulators were used to produce 20 random, image dependent deformations for 20 transversal slices extracted from 3-D MRI images. The deformations were normalized, in order to use them for simulating various degrees of anatomical differences, expressed by the maximum absolute initial displacement $|e_0^{MAX}| \in \{8 \text{ mm}, 10 \text{ mm}, 12 \text{ mm}\}$. T₂-weighted transversal images with 3% noise and 20% intensity nonuniformity (INU) were obtained from the Simulated Brain Database (SBD) [13] and after they were deformed, registrations to their corresponding artifact-free T1-weighted images were performed and the errors between the resulting and the initial deformations were measured. The residual root mean squared errors e_{RMS} were grouped for each case of simulated anatomical variability and their average values are presented in Tab. 2.

The results show that the presented multilevel block matching method is able to recover smooth synthetic deformations from TPSSim better than the more complex ones generated by RGsim. The best results were achieved when the 3rd-order B-splines were used as the kernel functions in the GPV interpolator employed in the construction of joint PDF estimate as well as in the regional matching.

Table 2 – Root mean squared error displacements achieved by the multilevel block matching technique on various initial misregistrations and with various setups in GPV interpolation kernel functions. The order of B-splines used in joint PDF estimate construction is signed as o_1 and the order of B-splines used in regional matching is signed as o_2 . The average computational time is also reported for each setup of the method.

$ e_0^{MAX} $ [mm]	e_0^{RMS} [mm]	e^{RMS} [mm]											
		o_1	o_2	o_1	o_2	o_1	o_2	o_1	o_2	o_1	o_2	o_1	o_2
		1	1	2	1	3	1	2	2	3	2	3	3
Comp. time [s]		100	104	115	169	178	300						
TPSSim													
5	2.47	0.59	0.57	0.56	0.51	0.52	0.51						
8	3.95	0.74	0.71	0.69	0.68	0.67	0.67						
10	4.93	0.91	0.89	0.86	0.85	0.82	0.82						
12	5.92	1.17	1.38	1.34	1.16	1.36	1.35						
RGsim													
5	2.30	0.93	0.87	0.85	0.79	0.77	0.75						
8	3.67	1.47	1.41	1.37	1.39	1.33	1.27						
10	4.59	2.19	2.17	2.09	2.05	2.07	1.98						
12	5.51	3.09	2.93	2.92	3.05	2.93	2.99						

4. DISCUSSION

Although the concept of block matching techniques is not new at all, this kind of registration algorithms is still in the

focus of research [14]. Here, it was adapted to the problem of multimodal intersubject registration of MRI brain images. The biggest limitation of block matching techniques is their high computational load which arises from the high amount of local optimization tasks. However, this drawback was solved e.g. in [15] by using parallel version of block matching on a cluster of computers. The high computational times reported here in Tab. 2 were achieved in a single-PC environment equipped with AMD Athlon 1.8 GHz processor and 2 GB RAM. The algorithms were implemented in MATLAB and C.

Comparing to another method for multimodal deformable registration presented in [6], similar registration quality was achieved here on smooth synthetic deformations, whereas worse results were obtained in recovering more complex deformations. This might be a result of more intensive regularization of the final displacement field. Besides the spatial deformation model, a considerable part of regularization is done here also in regional block matching where the point similarities are averaged over subimages.

In the field of computational neuroanatomy, the presented method showed to be applicable in spatial normalization which is performed in voxel-based morphometry, where global shape differences are suppressed and residual anatomical variability is then studied in voxel-by-voxel manner.

5. CONCLUSION

A multilevel block matching technique for deformable registration in computational neuroanatomy was presented. The multimodal character of the method makes it robust to tissue intensity variations which can be result of multimodality imaging as well as neuropsychological diseases or even normal aging.

The GPV interpolation concept, which was originally used for joint PDF estimation, was used here in regional matching. The influence of the kernel function used in GPV interpolation on the resulting registration quality was studied in experiments with simulated MRI brain image data and synthetic deformations. The quantitative evaluation showed that higher-order B-splines as the kernel functions in GPV interpolation framework give better results in registration quality than kernel functions with smaller support.

The proposed technique was stated to be suitable for voxel-based morphometry, where only gross intersubject anatomical differences should be suppressed by spatial normalization and the residual variability has to be preserved for following statistical parametric tests.

ACKNOWLEDGEMENT

This work was supported by the Czech Science Foundation, project no. 102/07/P263.

REFERENCES

- [1] A. Gholipour et al., "Brain functional localization: a survey of image registration techniques," *IEEE Transactions on Medical Imaging*, vol. 26, pp. 427–451, 2007.

- [2] J.P.W. Pluim, J.B.A. Maintz, M.A. Viergever, "Mutual-information-based registration of medical images: a survey," *IEEE Transactions on Medical Imaging*, vol. 22, pp. 986–1004, 2003.
- [3] T. Rohlfing, C. R. Maurer, D. A. Bluemke and M. A. Jacobs, "Volume-preserving nonrigid registration of MR breast images using free-form deformation with an incompressibility constraint," *IEEE Transactions on Medical Imaging*, vol. 12, pp. 730–741, 2003.
- [4] Y. Pauchard, M. R. Smith and M. P. Mintchev, "Modeling susceptibility difference artifacts produced by metallic implants in magnetic resonance imaging with point-based thin-plate spline image registration," in *Proceedings of 26th Annual International Conference of IEEE Engineering in Medicine and Biology Society*, 2004, pp. 1766–1769.
- [5] E. D'Agostino, F. Maes, D. Vandermuelen and P. Suetens, "A viscous fluid model for multimodal non-rigid image registration using mutual information," *Medical Image Analysis*, vol. 7, pp. 541–548, 2003.
- [6] D. Schwarz et al., "A deformable registration method for automated morphometry of MRI brain images in neuropsychiatric research," *IEEE Transactions on Medical Imaging*, vol. 26, pp. 452–461, 2007.
- [7] J. Tsao, "Interpolation artifacts in multimodality image registration based on maximization of mutual information," *IEEE Transactions on Medical Imaging*, vol. 22, pp. 854–864, 2003.
- [8] F. Maes et al., "Multimodality image registration by maximization of mutual information," *IEEE Transactions on Medical Imaging*, vol. 16, pp. 187–198, 1997.
- [9] H. Chen H. and P.K. Varshney, "Mutual information-based CT-MR brain image registration using generalized partial volume point histogram estimation," *IEEE Transactions on Medical Imaging*, vol. 22, pp. 1111–1119, 2003.
- [10] C. Studholme et al., "Deformation tensor morphometry of semantic dementia with quantitative validation," *NeuroImage*, vol. 21, pp. 1387–1398, 2004.
- [11] P. Rogelj and S. Kovacic, "Point Similarity Measure Based on Mutual Information," *Lecture Notes in Computer Science*, vol. 2717, pp. 112–121, 2003.
- [12] M. Fornefett, K. Rohr and H. S. Stiehl, "Radial basis functions with compact support for elastic registration of medical images," *Image Vision Comput.*, vol. 19, pp. 87–96, 2001.
- [13] D. L. Collins et al., "Design and construction of a realistic digital brain phantom," *IEEE Transactions on Medical Imaging*, vol. 17, pp. 463–468, 1998.
- [14] U. Malsch, C. Thieke, P.E. Huber and R. Bendl, "An enhanced block matching algorithm for fast elastic registration in adaptive radiotherapy," *Physics In Medicine and Biology*, vol. 51, pp. 4789–4806, 2006.
- [15] O. Clatz et al., "Robust nonrigid registration to capture brain shift from intraoperative MRI," *IEEE Transactions on Medical Imaging*, vol. 24, pp. 1417–1427, 2005.